Supporting Information to

2-Aminobenzazolium Chlorocuprate(II) Complexes for Memristive Devices: Structural Studies, Synaptic Plasticity, and Random Number Generation

by

Andrzej Sławek,[a,*] Gisya Abdi,[a] Ewelina Cechosz,[a] Marta Janioł,[a] Sidra Muzaffar,[a] Krzysztof Mech,[a] Alexey Maximenko,[b] Anna Dołęga,[c] Takuya Matsumoto,[d] and Konrad Szaciłowski[a]

[a] Academic Centre for Materials and Nanotechnology, AGH University of Krakow, ul. Kawiory 30, 30-055 Kraków, Poland

[b] National Synchrotron Radiation Centre SOLARIS, Jagiellonian University, ul. Czerwone Maki 98, 30-392 Kraków, Poland

[c] Department of Inorganic Chemistry, Chemical Faculty, Gdansk University of Technology, ul. Narutowicza 11/12, 80-233 Gdańsk, Poland

[d] Department of Chemistry, Graduate School of Science, Osaka University, 1-1 Machikaneyama, Osaka, Toyonaka, 560-0043, Japan

Contents

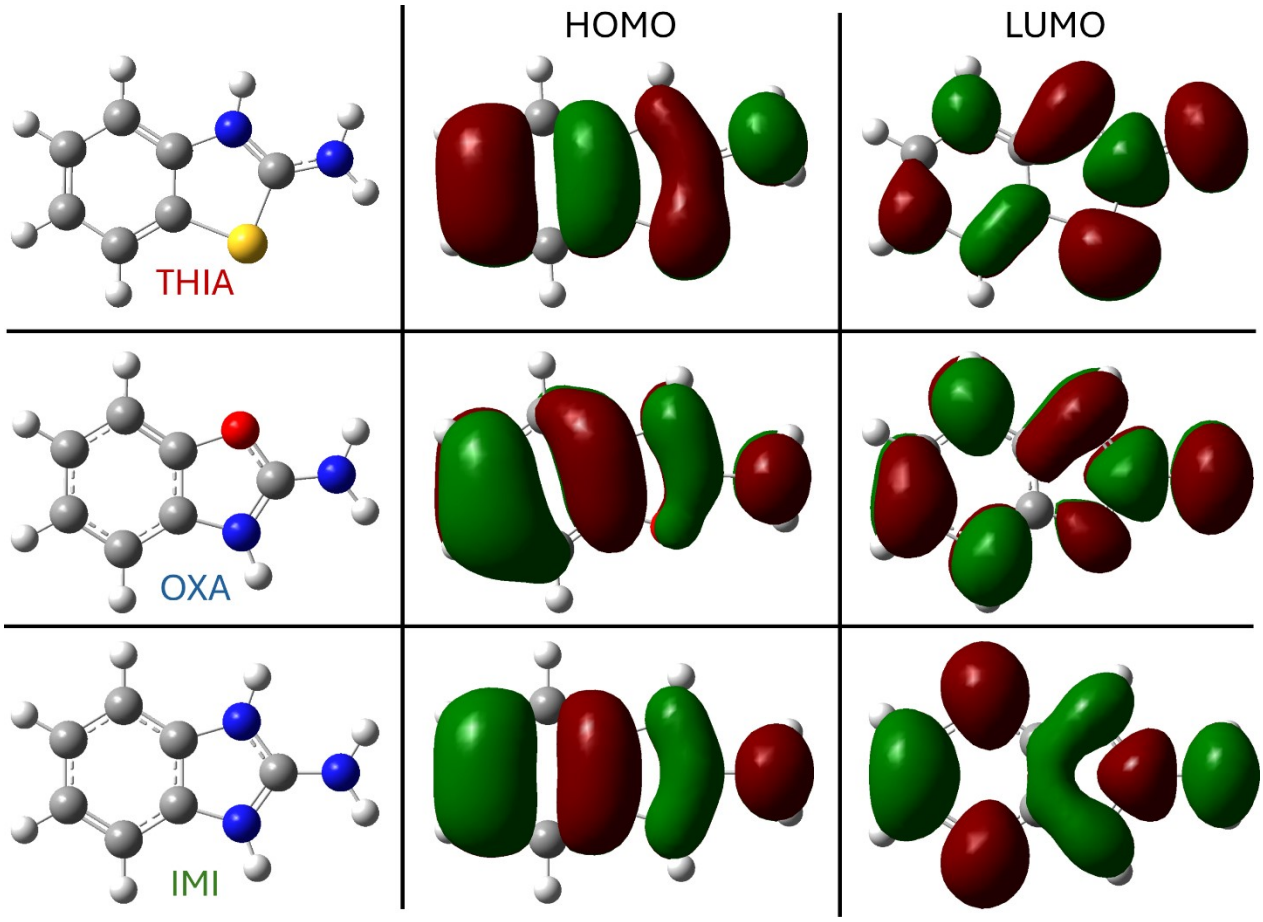

Figure S1. The optimized geometries of the studied cations: **THIA** (top), **OXA** (middle), and **IMI** (bottom) are presented on the left side together with the corresponding HOMO (middle) and LUMO (right) frontier orbitals.

Table S1. Crystal and refinement data for the studied compounds.

Compound	OXA	THIA	IMI
Empirical formula	$C_{14}H_{14}Cl_4CuN_4O_2$	$C_{14}H_{14}Cl_4CuN_4S_2$	$C_{21}H_{21}Cl_5CuN_9$
Formula weight (g mol^{-1})	475.63	507.75	640.26
Wavelength (Å)	0.71073	0.71073	1.54186
Temperature (K)	120(2)	120(2)	120(2)
Crystal system	monoclinic	monoclinic	hexagonal
Space group	*C* 2/*c*	*P* 2_1/*c*	*P* -6
***a* (Å)**	17.4866(7)	6.9352(3)	13.6407(5)
***b* (Å)**	8.7279(5)	9.7138(4)	13.6407(5)
***c* (Å)**	12.0090(5)	13.9419(6)	8.1276(2)
***α* (°)**	90	90	90
***β* (°)**	96.365(3)	97.775(3)	90
***γ* (°)**	90	90	120
Volume (Å^3)	1821.53(15)	930.59(7)	1309.68(10)
Z	4	2	2
Calculated density (g cm^{-3})	1.734	1.812	1.624
Crystal size (mm)	0.380x 0.307x 0.227	0.124x 0.097x 0.077	0.308x 0.221x 0.161
Absorption coefficient (mm^{-1})	1.802	1.978	1.37
***F*(000)**	956	510	648
θ range (°)	2.34 to 29.64	2.563 to 29.203	2.51 to 29.52
Limiting indices	-23≤h≤23	-8≤h≤9	-18≤h≤9
	-11≤k≤11	-13≤k≤13	0≤k≤18
	-16≤l≤16	-19≤l≤19	0≤l≤11
Reflections collected / unique/unique [*I>2σ(I)*]	11459, 2463, 2167	11965, 2512, 2302	23931, 2521, 2083
R_{int}	0.0303	0.0215	0.0184
Completeness to θ_{max} (%)	99.3	99.1	-
Data / restraints / parameters	2463 / 0 / 126	2512 / 0 / 127	-
Goodness-of-fit on F^2	1.050	1.078	-
Final R indices [*I>2σ(I)*]	R_1 = 0.0356	R_1 = 0.0267	-
	wR_2 = 0.0898	wR_2 = 0.0635	-
R indices (all data)	R_1 = 0.0432	R_1 = 0.0306	-
	wR_2 = 0.0965	wR_2 = 0.066	-
Largest diff. peak and hole (e Å^{-3})	0.443/-0.828	0.410/-0.605	-
CCDC deposition number	2471018	2471019	-

Table S2. Selected bond lengths and angles in the studied compounds. The data for **OXA** and **THIA** come from the diffraction experiment, and the data for **IMI** were optimized using DFT calculations.

Compound	OXA	THIA	IMI
		Bond lengths [Å]	
Cu1/Cu2*–Cl1/Cl6*	2.2399(5)	2.2718(4)	2.331/2.325
Cu1/Cu2*–Cl2/Cl7*	2.2580(6)	2.2745(4)	2.341/2.334
Cu1/Cu2*–Cl3/Cl8*			2.426/2.398
Cu1/Cu2*–Cl4/Cl9*			2.401/2.397
Cu1/Cu2*–Cl5/Cl10*			2.406/2.422
		Bond angles [°]	
Cl1–Cu1–Cl2	126.269(19)	89.628(16)	179.29
Cl1–Cu1–Cl1^{i}/Cl3*		179.999(18)	91.19
Cl3*/Cl1^{ii} –Cu1–Cl1/Cl4*	102.76(3)		118.14
Cl1^{ii} –Cu1–Cl2	101.972(19)		
Cl1^{ii} –Cu1–Cl2^{ii}	126.27(2)		
Cl1 –Cu1–Cl2^{ii}	101.971(19)		
Cl2^{ii} –Cu1–Cl2^{ii}	100.40(3)		

***IMI**; ^{i} –x+1, -y+2, -z+1; ^{ii} –x+1, y, -z+0.5

Table S3. Hydrogen bonds parameters for **OXA** and **THIA**.

Compound	H-Bond	D–H [Å]	H···A [Å]	D···A [Å]	D–H–A [°]
OXA	N1–H1···Cl1	0.78(4)	2.46(4)	3.184(2)	154(3)
	N2–H2A···Cl1[i]	0.83(4)	2.90(4)	3.325(2)	114(3)
	N2–H2A···Cl2[ii]	0.83(4)	2.51(3)	3.267(2)	151(3)
	N2–H2B···Cl2[iii]	0.92(3)	2.33(3)	3.228(2)	164(3)
THIA	N1–H1···Cl1	0.73(2)	2.41(2)	3.1327(17)	171.1(19)
	N2–H2A···Cl1[iv]	0.83(3)	2.69(3)	3.3535(18)	138(2)
	N2–H2A···Cl2[iv]	0.83(3)	2.51(3)	3.2406(18)	146(3)
	N2–H2B···Cl2[v]	0.82(3)	2.38(3)	3.1957(19)	174(3)

[i] –x+1, -y+1, -z+1; [ii] –x+1, y, -z+0.5; [iii] x, -y, z+0.5; [iv] x, -y+1.5, z-0.5; [v] –x+1, -y+2, -z+1

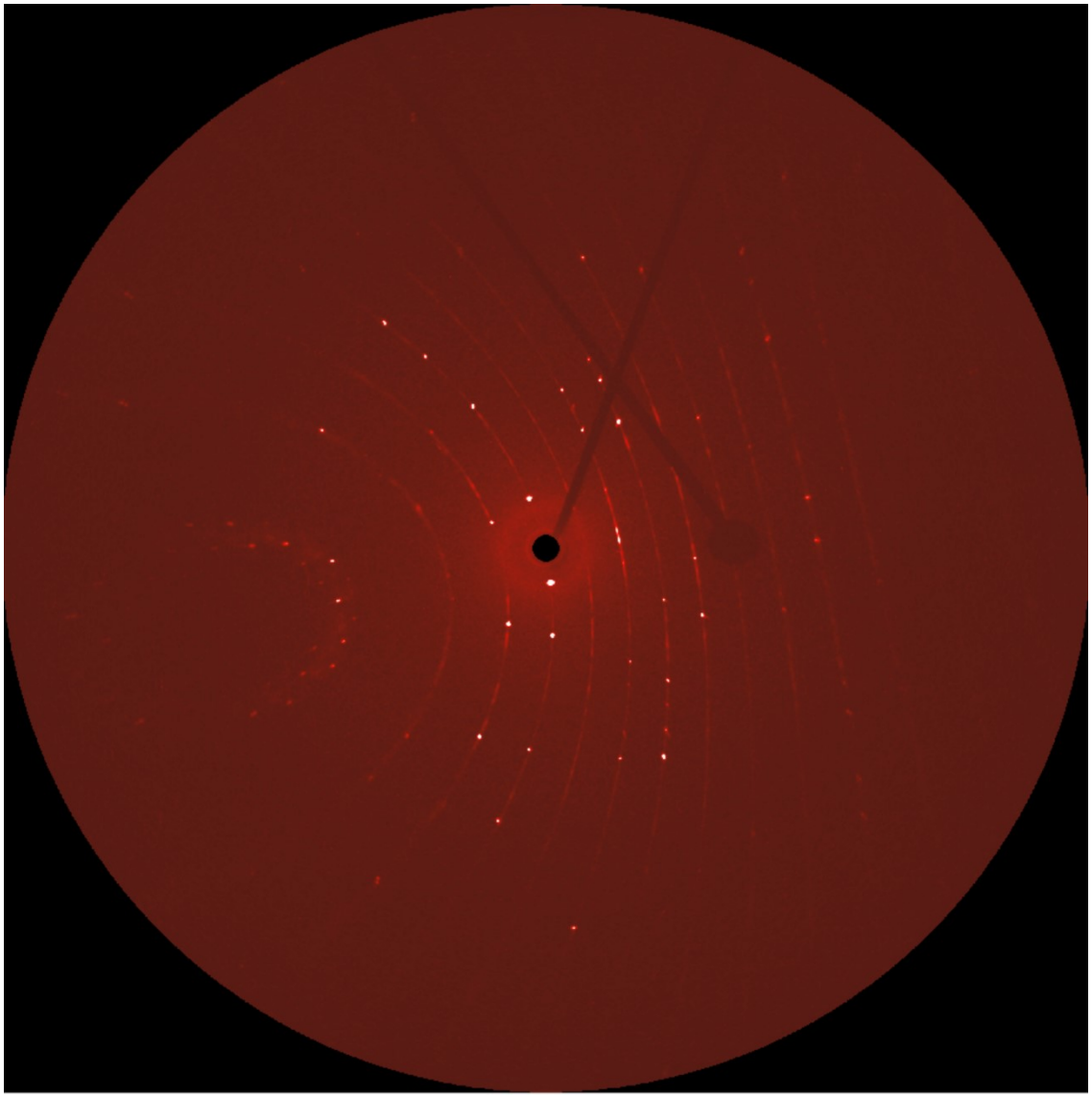

Figure S2. One of the frames registered during the diffraction measurement of crystals of **IMI**.

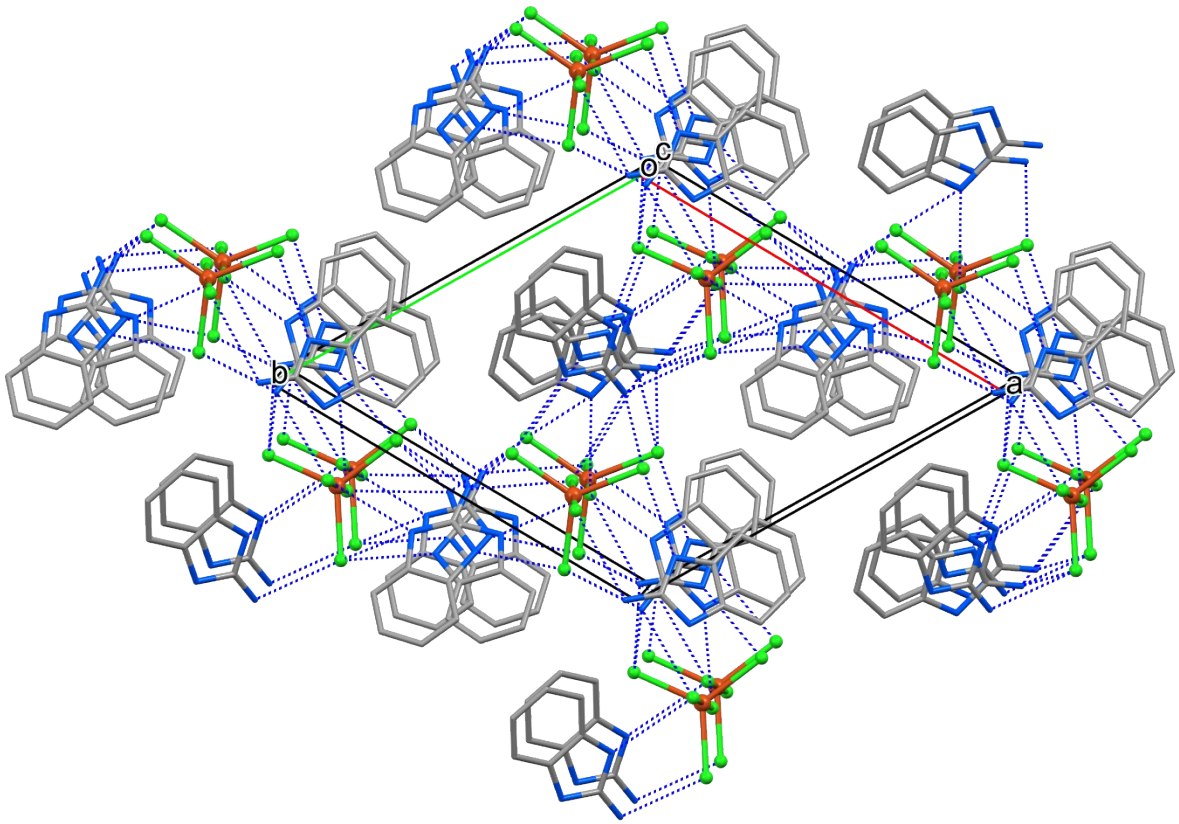

Figure S3. Hydrogen bonding network in **IMI**.

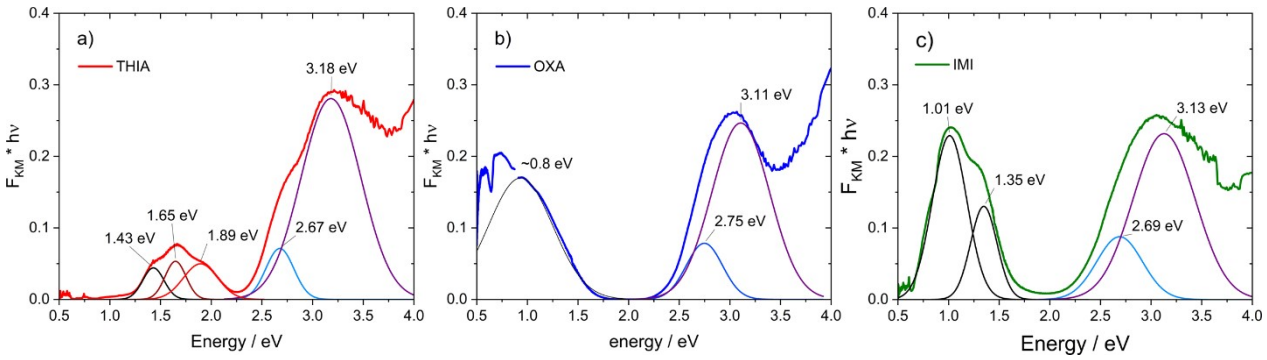

Figure S4. Deconvolution of the UV-Vis-NIR absorption spectra for **THIA** (a), OXA (b), and **IMI** (c) chlorocuprate(II) complexes into their Gaussian components. Spectra were measured as reflectance of powders in $BaSO_4$.

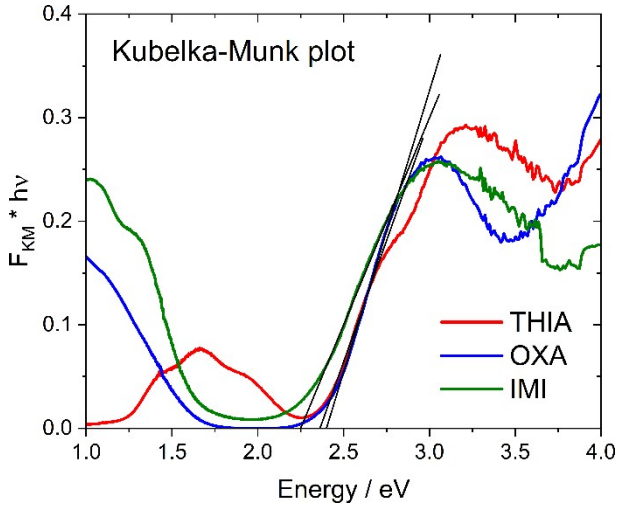

Figure S5. Kubelka-Munk function versus energy for determination of band gap for the studied **THIA**, **OXA**, and **IMI** chlorocprates(II). The band gaps are equal to

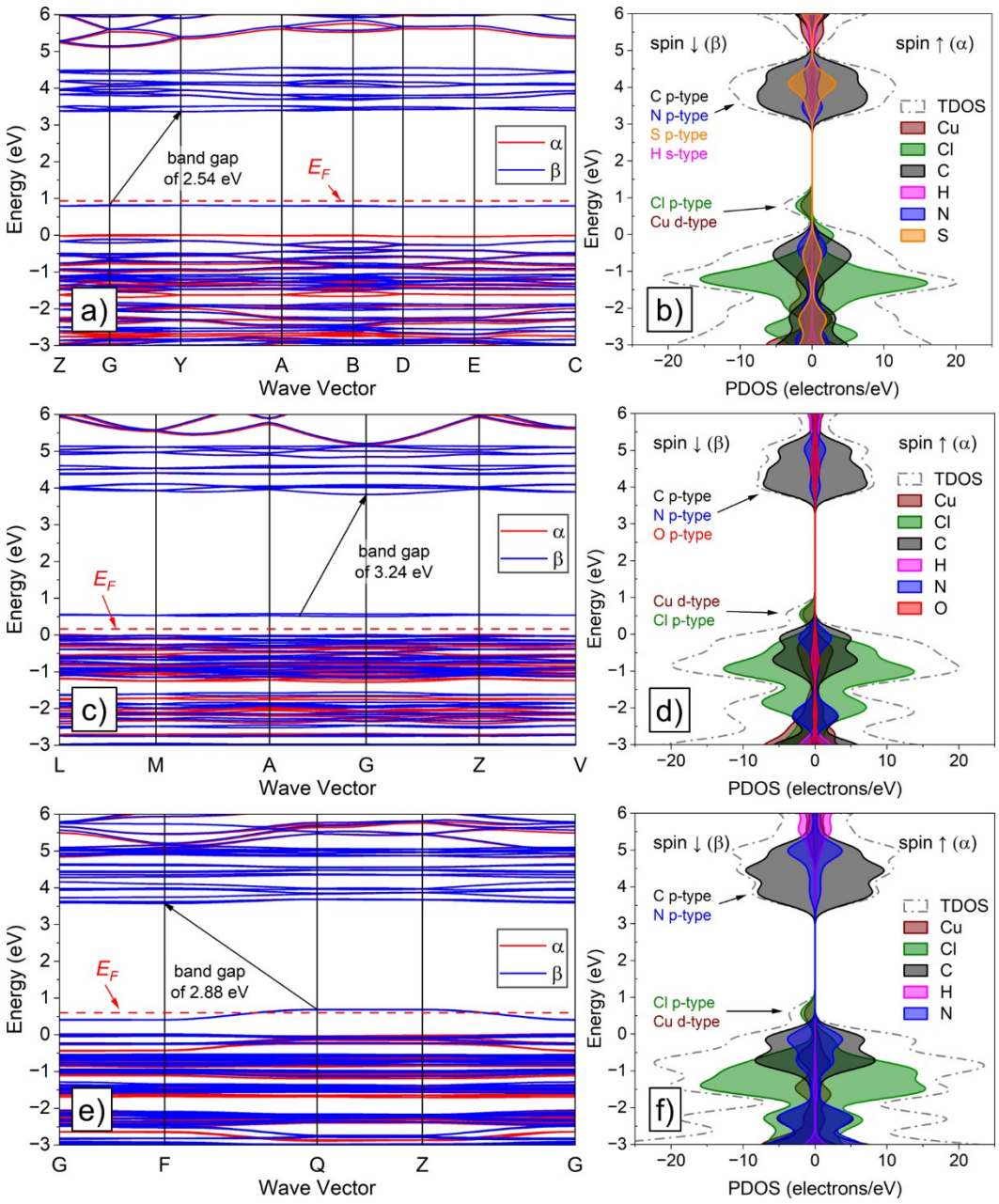

Figure S6. DFT-calculated band structures (left) and PDOS (right) for the studied chlorocuprate (II) complexes with **THIA** (a), **OXA** (b), and **IMI** (c). The band gaps are 2.54 eV, 3.24 eV, and 2.88 eV, respectively. The Fermi level is marked with a red dotted line.

Table S6. The values of experimental and DFT-calculated band gaps for the studied 2-aminobenzazoles chlorocuprates(II) complexes: **THIA** (a), **OXA** (b), and **IMI** (c) are compared with gap types and effective masses of holes (m_h) and electrons (m_e), as well as intrinsic carrier concentrations (n_i).

	Exp. Band gap (eV)	**Theor. band gap (eV)**	**Gap type**	**m_h/m_0**	**m_e/m_0**	**n_i (cm^{-3})**
THIA	2.36	2.54	Indirect	31.9	9.7	7.5×10^{-1}
OXA	2.40	3.24	Indirect	7.5	1.5	8.8×10^{-9}
IMI	2.25	2.88	Indirect	3.3	3.6	9.0×10^{-5}

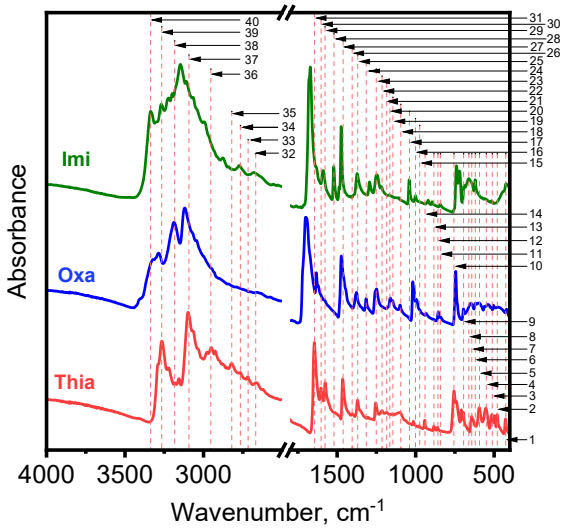

Figure S7. FT-IR spectra recorded for the powdered samples of the studied chlorocuprate(II) complexes with 2-aminobenzazoles **THIA**, **OXA**, and **IMI**. The lines corresponding to particular assignments were centered at positions coloured in Table S4 with red colour.

Table S4. Assignments of peaks observed in FT-IR spectra recorded for **THIA**, **OXA**, and **IMI** samples are presented in **Figure S7**.

Peak no	Position, cm^{-1}			Assigment	Ref*
	Thia	Oxa	Imi		
1	426	421	420	(N–CN) wagging	1
2	480	–	–	(C-C) deformation, (C–S–C) in-plane bending	1-2
3	512	503	514	C–C–C out of plane bending	1
4	550	536	–	(N-C) deformation	2
5	593	593	–	(C-S) stretching (C–C–C) out-of-plane bending	1-2
6	–	620	620	(C–C–C) out-of-plane bending	1
7	642	–	–	(C-S) stretching	2
8	–	649	661		
9	701	695	695	(C-N-H) bending	2
10	756	743	739	(C-N-H) bending	2
11	–	842	842		
12	858	857	–	(C-N-H) bending	2
13	884	883	893	(C-N) asymmetric stretching	2
14	940	930	919	(C-C-H) bending	2
15	974			(C-H) out-of-plane bending	1
16		991	1001	(C-C-H) bending	2
17	1014	1019	1039	(C-H) out-of-plane bending	1
18	1095	1098	1107	(C-C-H) bending	2
19	1150	1145	1151	(C-H) in-plane bending	1
20	–	1164	1164	(C-H) in-plane bending	1
21	1184			(C-H) in-plane bending	1
22	1214		1215	(C-H) in-plane bending	1
23	1251	1247	1245	(C-C-H) bending (C-H) in-plane bending	1-2
24	1303	1315	1294	(C-C) stretching	1
25	1369	1377	1374	(C=C) asymmetric stretching	2
26	1404			(C-C) stretching	1
27	1462	1474	1474	(N-H) bending	2

28	–	–	1520	(NH_2) symmetric bending	[2]
29	1577	1575	1588	(NH_2) symmetric bending	[2]
30	1602	1633		(C=N) stretching	[1]
31	1644	1696	1672	(NH_2) asymmetric bending	[2]
32	2667	–	2679		
33	2716	–	–		
34	2765	–	2765		
35	2820	–	2876		
36	2953	–	2994	(C-H) stretching	[2]
37	3093	3120	3141	(N-H) stretching	[2]
38	–	3184	–	(NH_2) symmetric stretching	[2]
39	3266	3288	3270	(NH_2) symmetric stretching	[2]
40	–	–	3337	(NH_2) asymmetric stretching	[2]

* Kessentini et al.,[2] Sathyanarayanmoorthi et al. and [1].

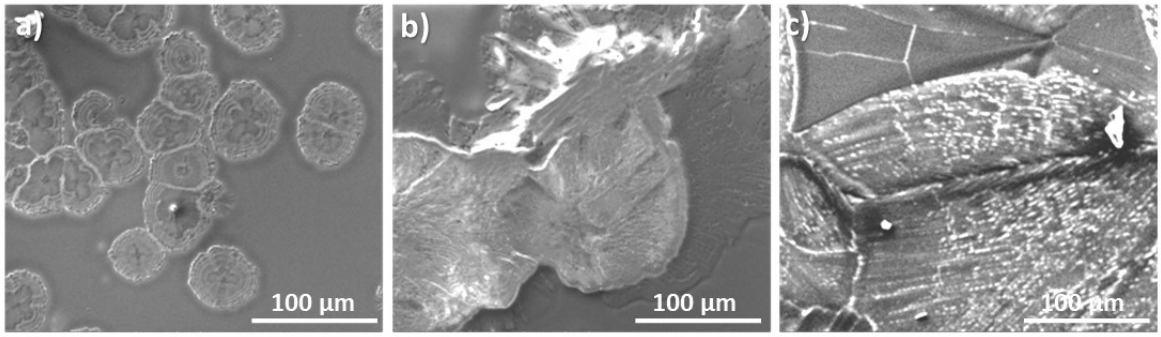

Figure S8. SEM images of the studied layers of chlorocuprate (II) complexes with 2-aminobenzazolium: a) **THIA**, b) **OXA**, and c) **IMI** on ITO.

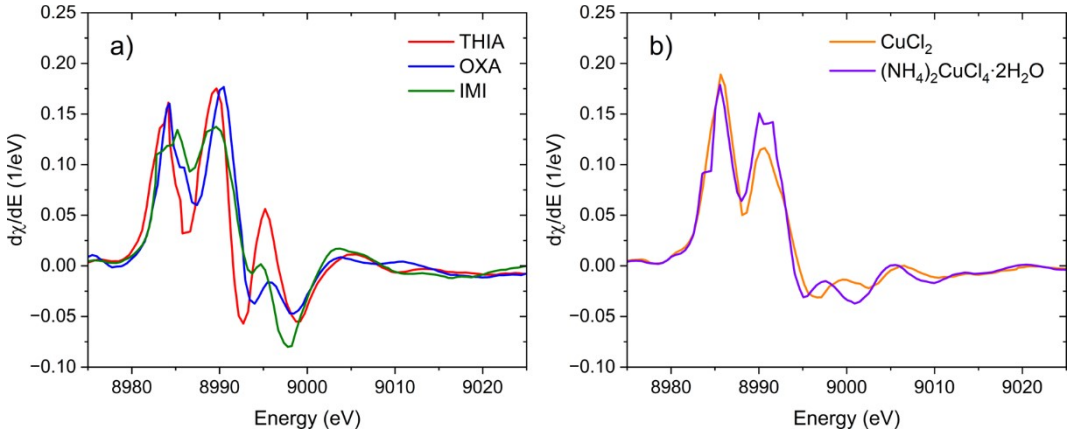

Figure S9. Cu K-edge spectra derivative with respect to energy for the 2-aminobenzazolium chlorocuprate(II) complexes **THIA**, **OXA**, and **IMI** (a) and the reference compounds $CuCl_2$ and $(NH_4)_2CuCl_4{\cdot}H_2O$.

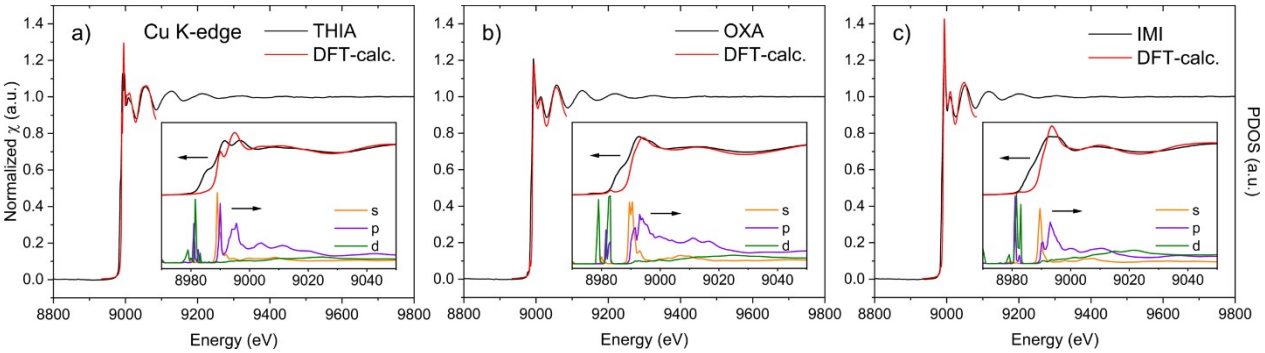

Figure S10. Full range Cu K-edge spectra of the studied 2-aminobenzazolium chlorocuprate(II) complexes: **THIA** (a), **OXA** (b), and **IMI** (c). Close-ups of the XANES region with the DFT-calculated spectra are presented in the inset figures.

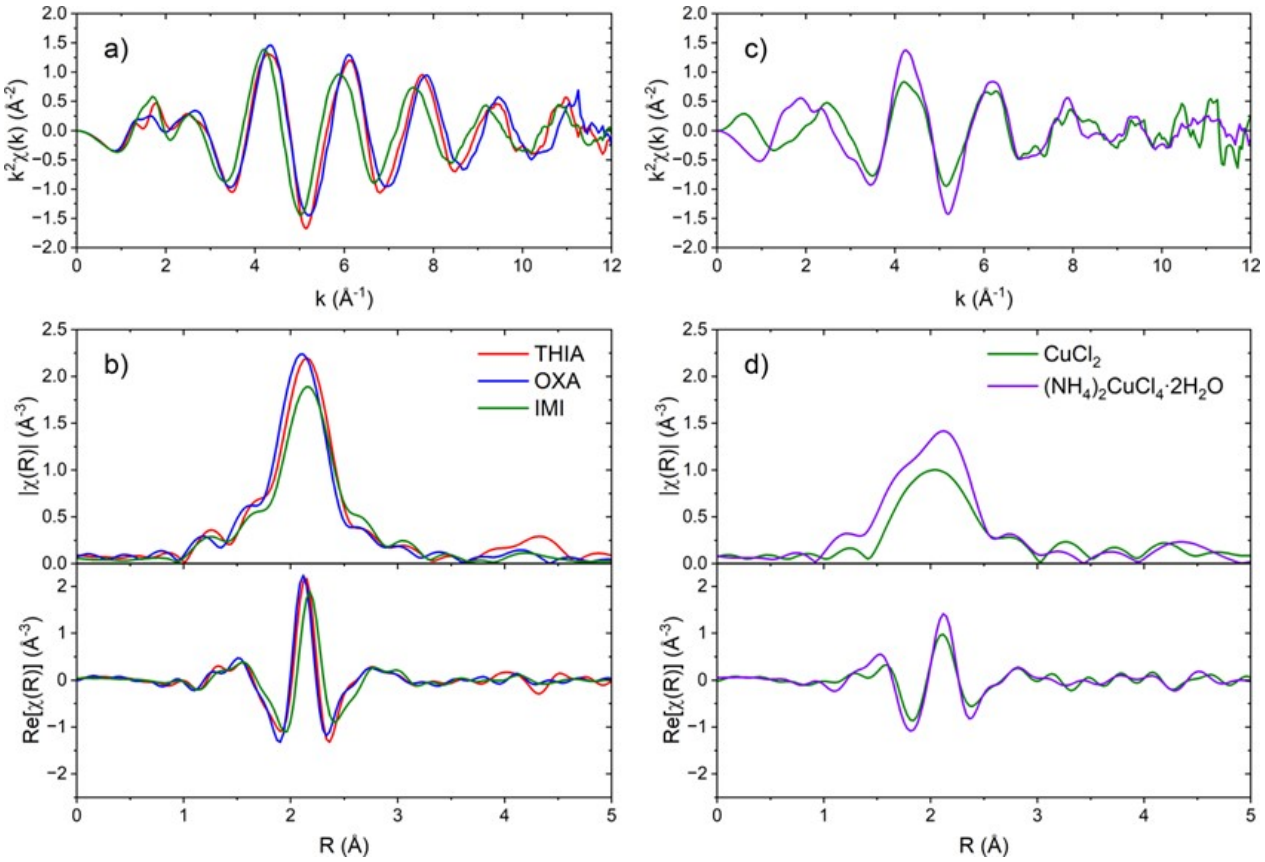

Figure S11. Cu K-edge EXAFS $\chi(k)k^2$ (a,c) and their Fourier transforms (b,d) for the 2-aminobenzazolium chlorocuprate(II) complexes: **THIA**, **OXA**, and **IMI** (a,b) and the reference compounds $CuCl_2$ and $(NH_4)_2CuCl_4{\cdot}H_2O$ (c,d).

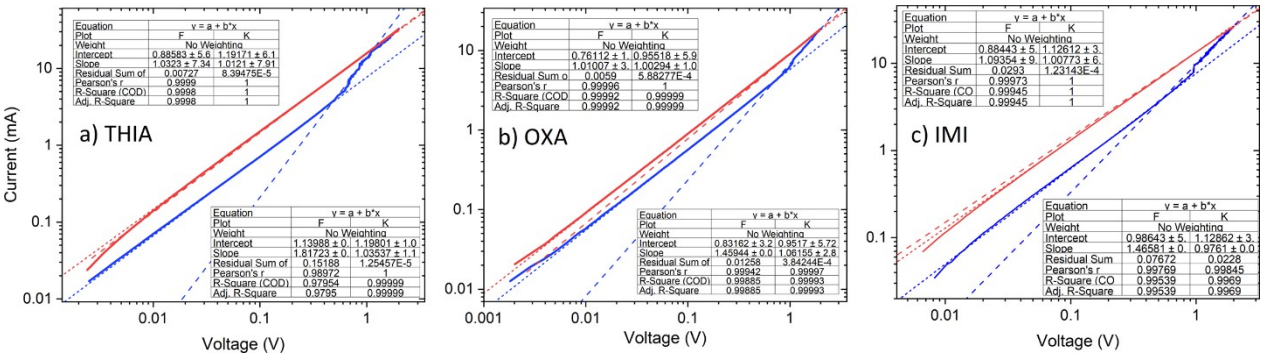

Figure S12. Log-log current−voltage characteristics of memristive devices based on the studied 2-aminobenzazolium chlorocuprate(II) complexes: **THIA** (a), **OXA** (b), and **IMI** (c). The scans were recorded at a rate of 25 mV/s.

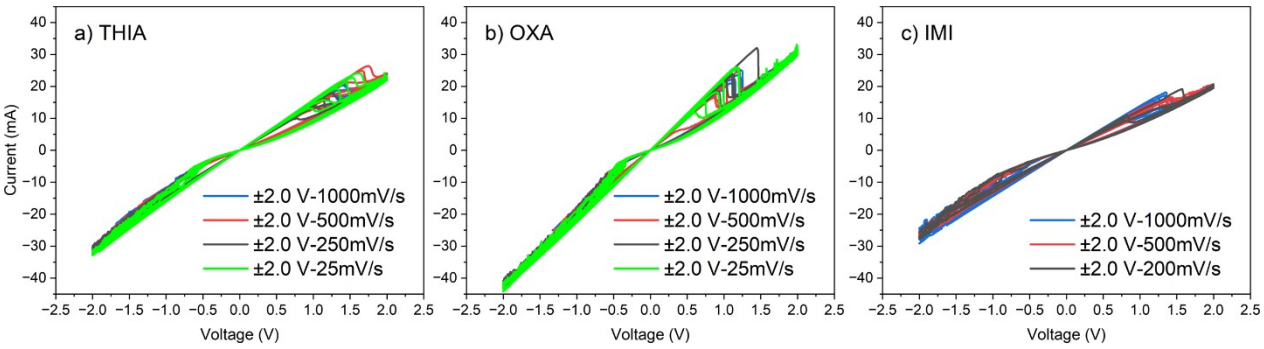

Figure S13. Current−voltage characteristics of memristive devices with different scan rates based on the studied 2-aminobenzazolium chlorocuprate(II) complexes: **THIA** (a), **OXA** (b), and **IMI** (c).

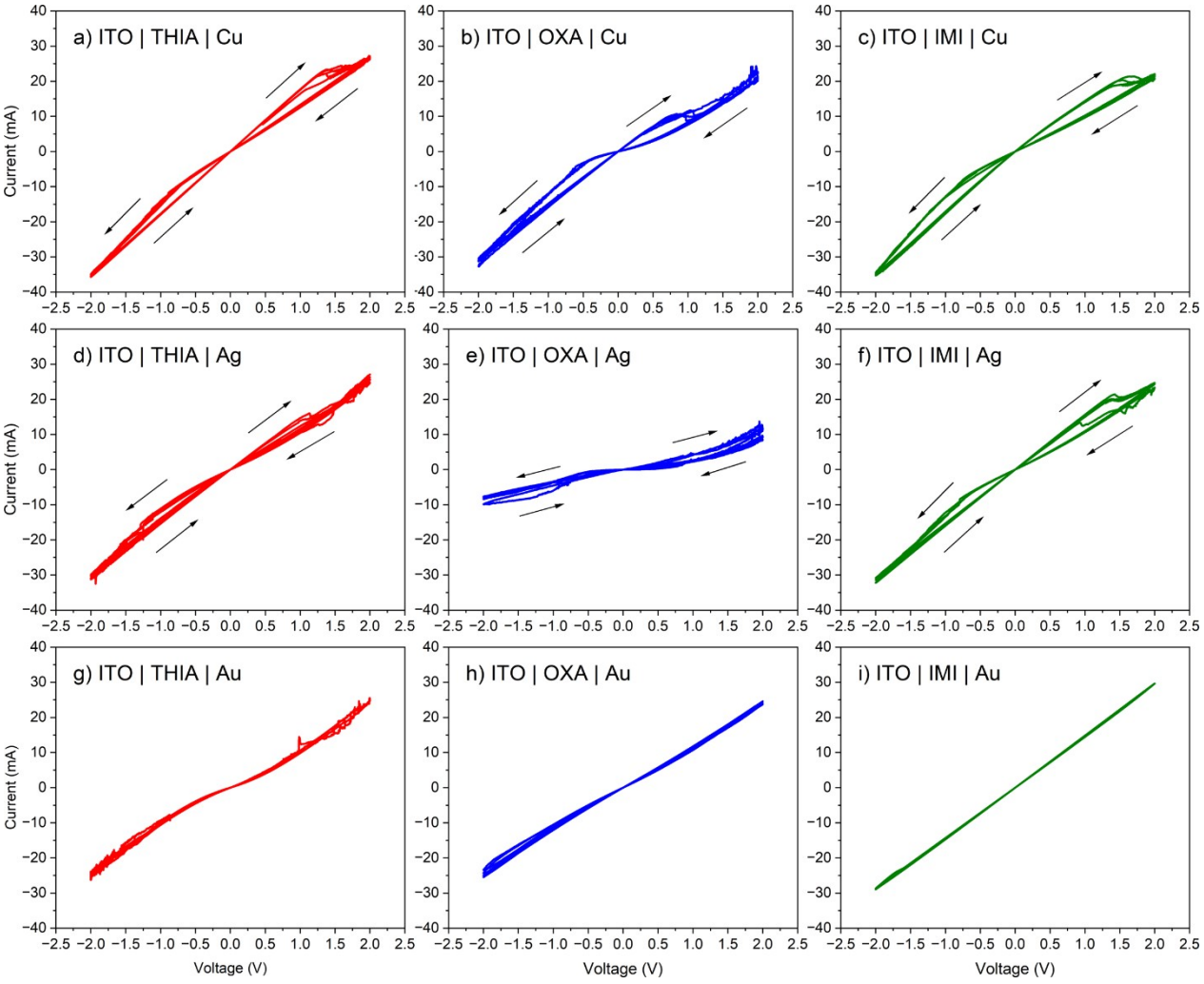

Figure S14. Current−voltage characteristics of memristive devices based on the studied 2-aminobenzazole chlorocuprates(II) complexes: **THIA** (a), **OXA** (b), and **IMI** (c) with different top electrodes: Cu (a-c), Ag (d-f), and Au (g-i).

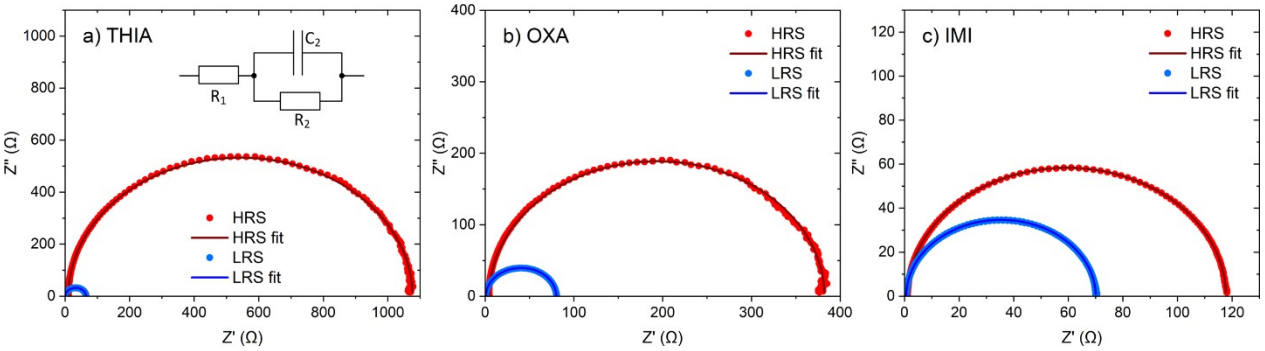

Figure S15. Nyquist plots showing experimental (points) and simulated (lines) results from electrochemical impedance spectroscopy (EIS) for the studied devices based on 2-aminobenzazoles chlorocuprates(II) complexes: **THIA** (a), **OXA** (b), and **IMI** (c) for LRS and HRS. The inset of a) shows the equivalent circuit model used for the simulations.

Table S5. Summary of the fitting parameters determined based on recorded EIS spectra for the studied devices based on 2-aminobenzazoles chlorocuprates(II) complexes: **THIA** (a), **OXA** (b), and **IMI** (c) complexes for low (LRS) and high resistance state (HRS), respectively. R_1 is the electrode (series) resistance, R_2 is the thin film (parallel) resistance, and C_1 is the thin film capacitance (parallel).

	R_1 (series, electrode)		R_2 (parallel, thin film)		C_1 (parallel, thin film)	
	LRS (Ω)	HRS (Ω)	LRS (Ω)	HRS (Ω)	LRS (F)	HRS (F)
THIA	0.57	10.3	64.4	1066	3.67×10^{-5}	2.12×10^{-6}
OXA	0.77	4.5	79.3	377.8	3.01×10^{-5}	5.88×10^{-6}
IMI	0.63	1.09	69.4	116.7	3.48×10^{-5}	2.04×10^{-5}

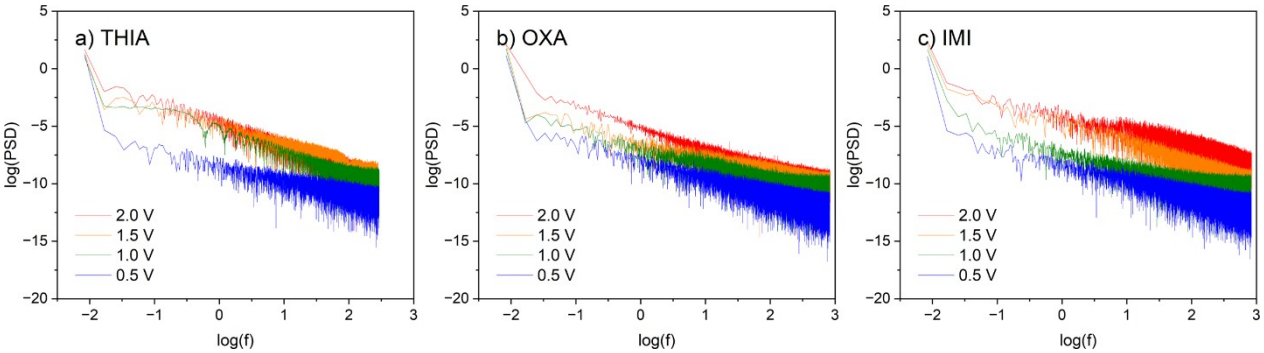

Figure S16 Power spectral density plot for the studied devices based on 2-aminobenzazole chlorocuprates(II) complexes: **THIA** (a), **OXA** (b), and **IMI** (c) subjected to voltages from 0.5 to 2 V.

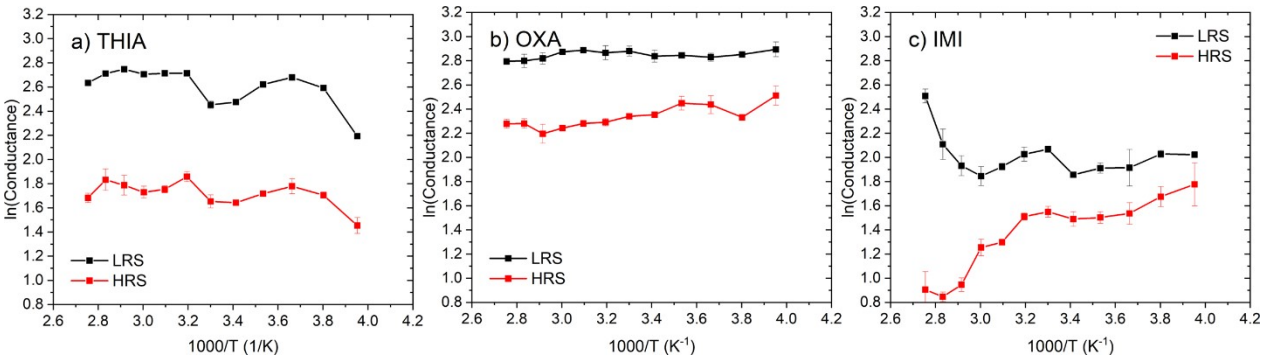

Figure S17. Arrhenius plots showing the temperature dependence of the natural logarithm of conductance (in mS) collected at +2 V (HRS) and -2 V (LRS).

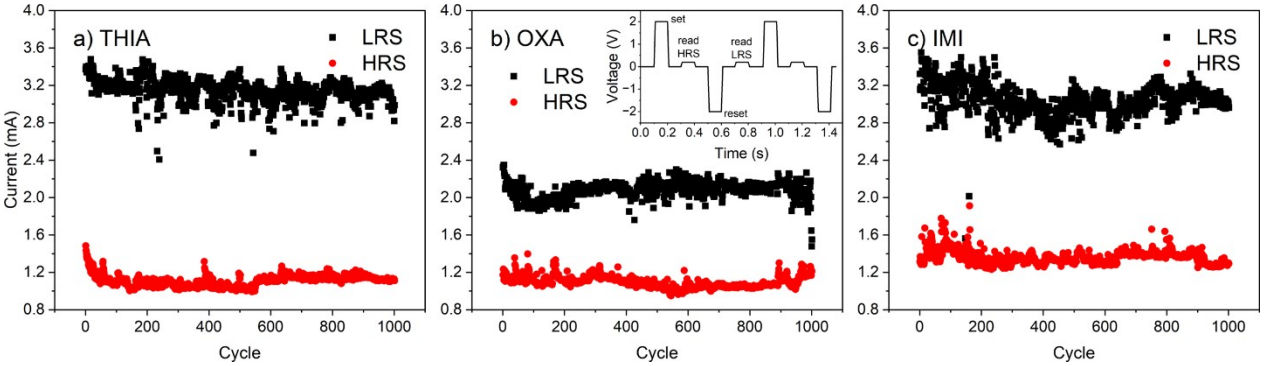

Figure S18. Chronoamperometric experiments showing repeated switching between HRS and LRS of devices based on 2-aminobenzazoles chlorocuprates(II) complexes: **THIA** (a), **OXA** (b), and **IMI** (c). The period of the cycle was 0.8 s. Read voltage equal to +0.2 V.

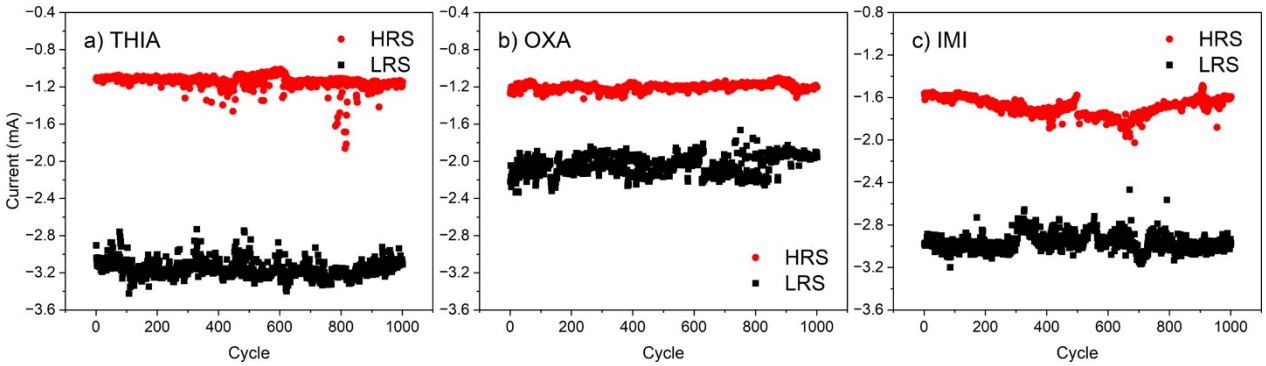

Figure S19. Chronoamperometric experiments showing repeated switching between HRS and LRS of devices based on 2-aminobenzazoles chlorocuprates(II) complexes: **THIA** (a), **OXA** (b), and **IMI** (c). The period of the cycle was 0.8 s. Read voltage equal to -0.2 V.

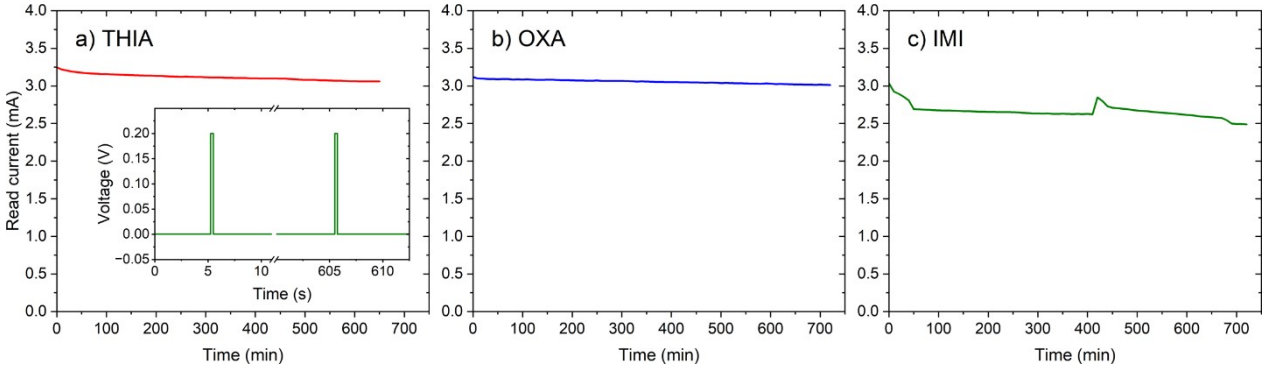

Figure S20. Chronoamperometric experiments showing retention time of LRS for the studied devices based on 2-aminobenzazoles chlorocuprates(II) complexes: **THIA** (a), **OXA** (b), and **IMI** (c). Figure a) inset shows the voltage change curve.

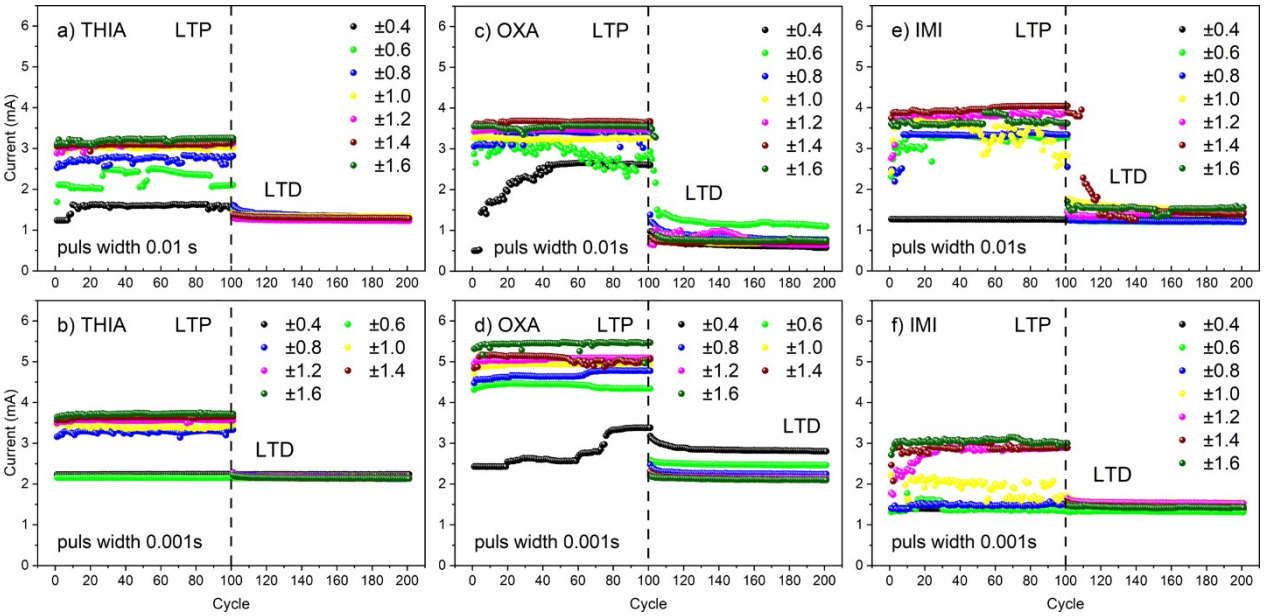

Figure S21. Potentiation (P) and depression (D) experiments for prepared devices based on 2-aminobenzazoles chlorocuprates(II) complexes: **THIA** (a, b), **OXA** (c, d), and **IMI** (e, f) with different pulse sequences of different widths (top: 0.001 s or bottom: 0.01 s) and amplitudes (in legend: 0.4-1.6 V).

References

1. Sathyanarayanmoorthi, V.; Karunathan, R.; Kannappan, V., Molecular Modeling and Spectroscopic Studies of Benzothiazole. *Journal of Chemistry* **2013,** *2013* (1), 258519.
2. Kessentini, A.; Belhouchet, M.; Abid, Y.; Minot, C.; Mhiri, T., Crystal structure, vibrational studies, optical properties and DFT calculation of bis 2-aminobenzothiazolium tetrachloridocuprate. *Spectrochimica Acta Part A: Molecular and Biomolecular Spectroscopy* **2014,** *122*, 476-481.